JOURNAL OF APPLIED ELECTROCHEMISTRY 19 (1989) 413–420

Impedance analysis of the lithium discharge in Li–$SOCl_2$ cells: synergetic effect of SO_2 and $LiAl(SO_3Cl)_4$

P. CHENEBAULT, D. VALLIN

S.A.F.T. Département des générateurs de technologies avancées, rue Georges Leclanché, B.P. 357, 86009 Poitiers, France

J. THEVENIN, R. WIART

Physique des Liquides et Electrochimie, Laboratoire Propre du C.N.R.S., Université Paris VI, 4 place Jussieu, 75252 Paris cedex 05, France

Received 22 March 1988; revised 28 November 1988

A study of the anodic discharge of the Li electrode in $LiAlCl_4/SOCl_2$ electrolyte shows the occurrence of a diffusion process mainly when the surface layer was formed in the presence of the inorganic additives SO_2 and $LiAl(SO_3Cl)_4$. A model of the electrode kinetics is proposed on the assumption that the ionic diffusion is hindered by the precipitation of the solute $LiAlCl_4$ at the bottom of holes formed in the compact polycrystalline LiCl surface layer by a dissolution–dilation mechanism.

1. Introduction

The performance advantages potentially available from $Li/SOCl_2$ primary batteries are adversely affected by an excessive growth of a LiCl surface layer on the Li anode during long-term storage. The morphological and kinetic properties of this surface layer are responsible for the voltage delay effect resulting in a cell voltage drop during the initial discharge. The recovery time to a normal operating voltage depends on the storage and discharge conditions.

Several approaches have been developed in order to reduce the voltage delay effect knowing that the surface layer is sensitive to the presence of various inorganic additives in the electrolyte [1–3]. Recently, the effectiveness of the additives SO_2 and $LiAl(SO_3Cl)_4$ has been demonstrated on both the voltage delay alleviation and the capacity retention of $SOCl_2/LiAlCl_4$ primary cells [4]. It has been shown that these inorganic additives have a synergetic effect on the morphological and electrical properties of the LiCl surface layer with consequent changes in the kinetics of the Li electrode during the cell storage. For example, the presence of the additives led to a reduction in the thickness of the surface layer, and a change in the shape and size of the microcrystals constituting this surface layer. It also led to a reduction in the polarization resistance at the equilibrium potential, and to a separation of the intergranular conduction and charge transfer processes involved in the surface layer considered as a polycrystalline solid electrolyte [5, 6].

During the discharge of the Li electrode, it has been generally observed that the formation of holes in the surface layer allows a direct contact between the electrode and the electrolyte [7]. Consequently, the surface layer cannot any longer be considered as a simple interphase having the properties of a polycrystalline solid electrolyte. The purpose of this paper is to study the combined influence of the additives SO_2 and $LiAl(SO_3Cl)_4$ on the kinetics of the anodic dissolution of the Li electrode covered by a LiCl surface layer. Accordingly, a study by means of electrode impedance spectroscopy has been performed in order to analyze the elementary processes involved in the system for steady state conditions under anodic polarization.

2. Experimental details

2.1. *Solutions*

Different solutions have been studied knowing that the optimal concentrations of each inorganic additive in $SOCl_2/LiAlCl_4$ have been defined according to a previous study on their influence on the voltage delay effect [4] and the properties of the surface layers [5]. These solutions have been named as follows:

the 'normal solution' (with only SO_2):

$$SOCl_2 + 1.35\,M\ LiAlCl_4 + 0.5\,M\ SO_2$$

the 'complete solution' (with SO_2 and $LiAl(SO_3Cl)_4$):

$$SOCl_2 + 1.35\,M\ LiAlCl_4 + 0.5\,M\ SO_2 + 0.017\,M\ LiAl(SO_3Cl)_4$$

2.2. *Electrochemical cell*

The special two-electrode cell has been described else-

0021-891X/89 $03.00 + .12

where [5]. The surfaces of the electrodes were disks of lithium (Foote Mineral Co., purity 99.9%). The surface area of the working electrode (0.07 cm^2) was much smaller than that of the counter electrode (28 cm^2). The hermetic and cylindrical cell container was made of stainless steel. The lithium electrode fitted in a glass tube was connected to the top of the cell container by using the central pin of a glass/metal seal.

2.3. *Kinetic studies*

Impedance measurements were performed for a wide frequency range (from 5×10^5 to 5×10^{-3} Hz) by using a frequency response analyzer (Solartron 1174) monitored by a microcomputer (Apple II). A galvanostat was used to superimpose a sinusoidal signal of a few $\mu A\ cm^{-2}$ at any polarization condition. According to the ratio between the surface areas of the electrodes, the measured impedance results mainly from the behavior of the working electrode. The impedance diagrams were automatically plotted in the complex plane on a printer connected to the microcomputer.

3. Results

In order to simplify the presentation of the results obtained by electrode impedance spectroscopy, a schematic view of the studied system must be considered, as shown in Fig. 1a. Assuming the presence of longitudinal holes formed through the whole surface layer during anodic polarization, the lithium electrode may be in contact with the liquid electrolyte on an active surface area, $(1 - \theta)$, and thus covered by the surface layer on a passive surface area, θ. Accordingly, as shown in Fig. 1b, the equivalent electrical circuit of the system comprises two main circuits in parallel, each component being proportional to the active and passive surface areas of the lithium electrode, respectively.

The properties of the active surface area, $(1 - \theta)$, can be represented by a Randles equivalent circuit. This circuit consists of the resistance, R_e, of the electrolyte filling the holes, and the classical circuit associated with the charge transfer and ionic diffusion processes occurring at the electrode–electrolyte interface. This circuit comprises the charge transfer resistance, R_t, and the diffusion impedance, Z_d (diffusion resistance, R_d) placed in series, and the double layer capacitance, C_{dl}, placed in parallel.

The properties of the passive surface area, θ, can be represented by the equivalent circuit of a solid electrolyte. By assuming that the intergranular conduction is the main process determining the behavior of the polycrystalline surface layer, as previously shown [5, 6], this equivalent circuit is practically equivalent to a grain boundary resistance, R_{gb}, placed in parallel with a grain boundary capacitance, C_{gb}. As the grain boundary resistance, R_{gb}, is many orders higher than the polarization resistance, $R_p = R_e + R_t + R_d$, of the active surface area, the circuit associated with the passive surface area can be reduced to the grain boundary capacitance, C_{gb}.

According to these hypotheses, the corresponding impedance diagram in the complex plane gives, at

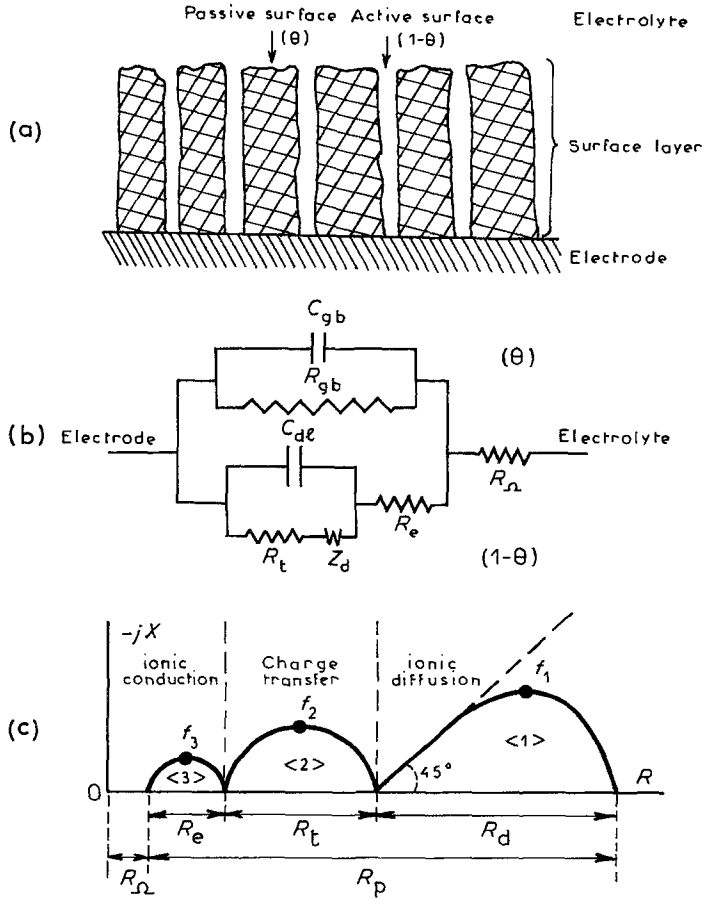

Fig. 1. (a) Schematic view of the electrode–layer system. (b) Equivalent electrical circuit of the system. (c) Corresponding impedance diagram in the complex plane.

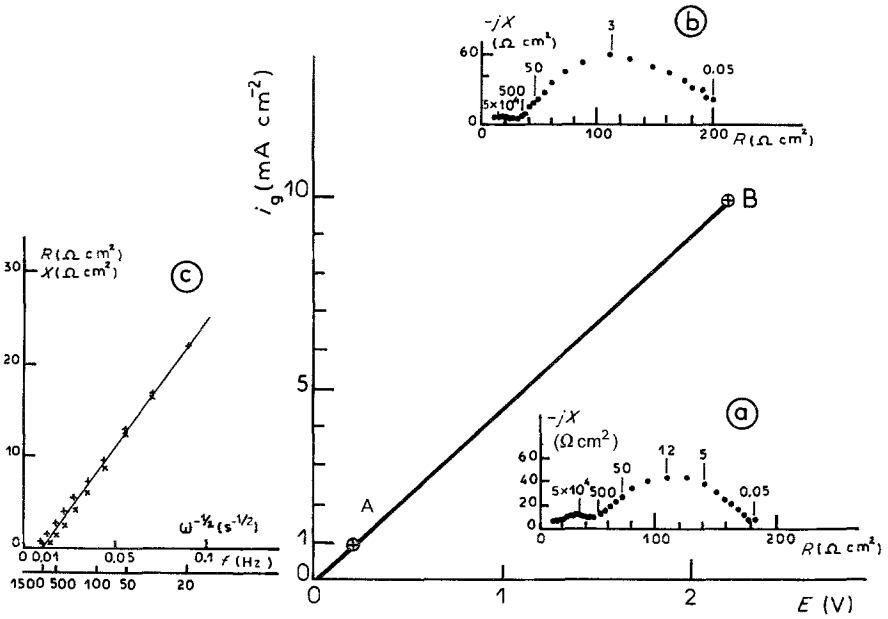

Fig. 2. Polarization curve for the case of the 'complete solution'. (a) and (b) Impedance diagrams obtained at different polarization points A and B, respectively. (c) Variation of the components R and X of the preceeding impedance diagram at the point B as a function of the inverse square root of the angular frequency, ω.

most, three capacitive semicircles or loops, the characteristic resistances of which are practically proportional to the active surface area of the lithium electrode. The indices ⟨1⟩, ⟨2⟩ and ⟨3⟩ have been used to identify these semicircles or loops in the low, medium and high frequency ranges, respectively. Considering the time constants generally attributed to the elementary processes, as shown in Fig. 1c, the loop ⟨1⟩ can be attributed to the diffusion process and associated with the diffusion resistance, R_d, the semicircle ⟨2⟩ to the charge transfer process and associated with the charge transfer resistance, R_t, and the semicircle ⟨3⟩ to the ionic conduction process and related to the electrolyte resistance, R_e. Moreover, the centers of the semicircles associated with these elementary processes lie under the real axis of the complex plane. This can be explained by statistical distributions of the time constants related to these processes taking place at the bottom of many holes with largely heterogeneous properties in the surface layer.

The kinetic properties of the system were studied for a large range of electrode potential, after a preliminary discharge at a current density of 1 mA cm^{-2} using a charge density of 0.25 C cm^{-2} (per unit of geometric surface area of the lithium electrode). This procedure was necessary to obtain a steady state kinetic behavior without any influence of the possible initial voltage delay effect. The impedance diagrams for different points of the polarization curves are shown in Figs 2 and 3, for the 'complete solution' and the 'normal solution', respectively. The synergetic effect of the inorganic additives is demonstrated by comparing the results concerning the relative importance of the processes involved during the anodic polarization.

For the 'complete solution' (with SO_2 and $LiAl(SO_3Cl)_4$), as shown in Fig. 2, the polarization resistance, R_p, remains practically constant over a large range of geometric current density, i_g, as expected considering the linear shape of the polarization curve. Considering that R_e is not observed on the

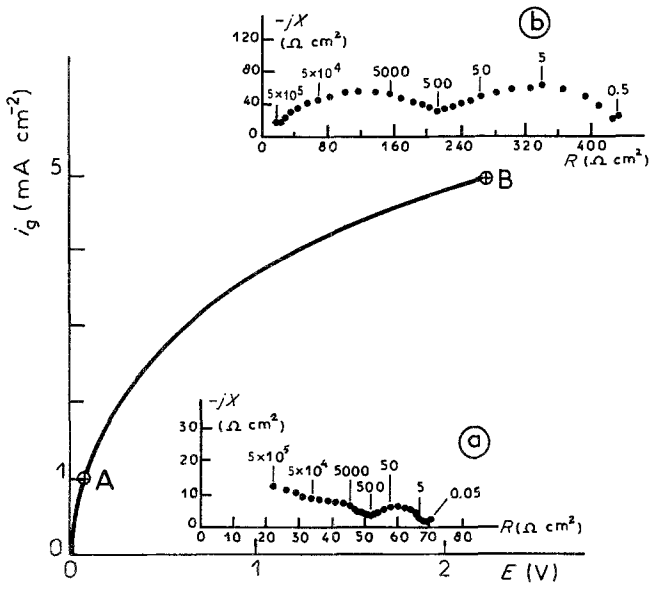

Fig. 3. Polarization curve for the case of the 'normal solution'. (a) and (b) Impedance diagrams obtained at different polarization points A and B, respectively.

impedance diagram (diagrams a and b in Fig. 2), the ratio R_d/R_t appears to increase slightly with the current density, and becomes about 5 at point B in Fig. 2 where the geometric current density, i_g, is $10\,mA\,cm^{-2}$ and the electrode potential, E, is 2.2 V vs Li. The semicircle ⟨2⟩, attributed to the charge transfer process, decreases while the current density increases, as currently observed for the case of an irreversible metal dissolution. The loop ⟨1⟩ exhibits a characteristic Warburg slope for the highest frequencies, and a semicircular shape for the low frequencies (diagrams a and b in Fig. 2). Accordingly, when the voltage delay effect is alleviated as a result of the synergetic effect of the inorganic additives, a diffusion process acting as the rate determining process is observed during the lithium discharge. The analysis of this diffusion impedance, Z_d, leads to the determination of the average values of three parameters: the diffusion resistance, R_d, about $150\,ohm\,cm^2$; the Warburg constant, σ, close to $250\,ohm\,cm^2\,s^{-1/2}$ (see drawing c in Fig. 2 for the variation of the impedance components R and X, as a function of the inverse square root of the angular frequency, ω); and the frequency, f^*, about 5 Hz (at the maximum of the imaginary component X of the complex diffusion impedance).

For the 'normal solution' (with only SO_2), as shown in Fig. 3, the polarization resistance, R_p, increases with the geometric current density, i_g, as expected by considering the asymptotic shape of the polarization curve. Knowing that R_t and R_e cannot be separated at high current densities, the ratio $R_d/(R_t + R_e)$ appears to increase up to about 1 at point B in Fig. 3 where the geometric current density, i_g, is $5\,mA\,cm^{-2}$ and the electrode potential, E, is 2.2 V vs Li. The loop ⟨1⟩ in the low frequency range, which is associated with an apparent capacitance of the order of $100\,\mu F\,cm^{-2}$ (diagrams a and b in Fig. 3), does not give any evidence of a classical Warburg diffusion process. However, it may be associated with an ionic diffusion process occurring for a large distribution in the parameters (size, length, structure) of the holes formed through the surface layer. Both the increasing ratio $R_d/(R_t + R_e)$ and the increasing diffusion resistance, R_d, with the current density still indicate that the ion transport becomes the rate determining process. On the other hand, the loop ⟨2⟩ does not correspond to a simple charge transfer process, since it appears that the resistance increases with the current density. Hence, this loop probably also reflects a passivation of the active surface area, a fast phenomenon in comparison with the ionic diffusion process and thereby not separated from the charge transfer process.

4. Kinetic model

To understand the coupling between the charge transfer and diffusion processes occurring during the anodic polarization for the 'complete solution', a more detailed presentation of the processes involved at the electrode/electrolyte interface is needed, as shown in Fig. 4a. At the equilibrium potential, the Li electrode surface is covered by a heterogeneous, but compact, surface layer. This layer comprised of LiCl microcrystals is due to the decomposition products of $SOCl_2$ which is chemically unstable in the presence of Li [5–8]. During anodic polarization, lithium tends to dissolve at the electrode–layer interface, and the transport of the generated ions is hindered by this surface layer. A dilation stress is thus imposed, causing the breakdown of the weak spots such as the grain boundaries of the polycrystalline surface layer. The propagation of such a dissolution dilation mechanism creates a number of more or less longitudinal holes through the surface layer [9]. Accordingly, the voltage delay effect can be directly related to the time necessary to form these holes, and the specific influence of the additives on this effect can be related to the existence of specific weak spots in the surface layer. The formation of holes is supposed to be easier when the LiCl surface layer has a heterogeneous structure, as observed in the presence of the inorganic additives

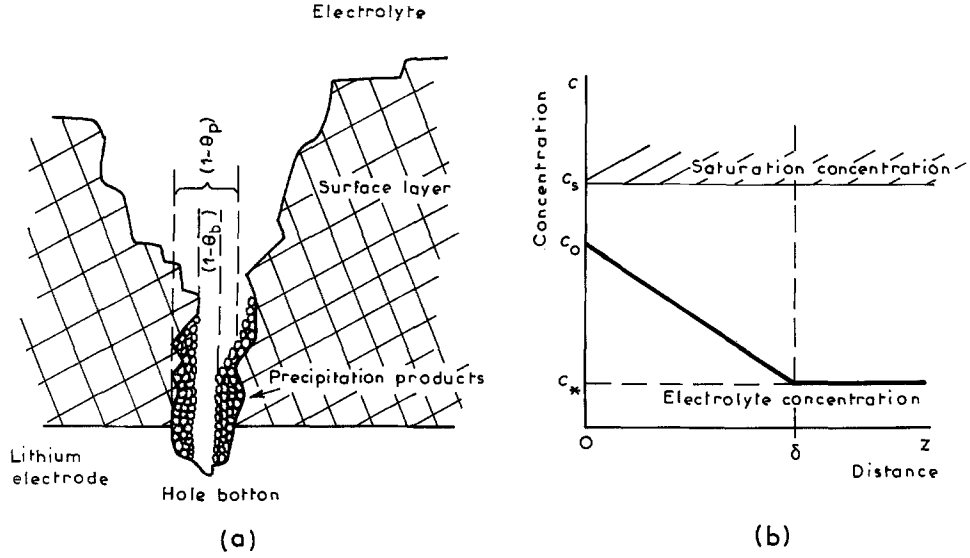

Fig. 4. (a) Schematic view of a typical hole inside the surface layer partially blocked by the precipitation products. (b) Variation of the ionic concentration as a function of the distance from the hole bottom.

SO_2 and $LiAl(SO_3Cl)_4$ in the $SOCl_2/LiAlCl_4$ electrolyte [5, 6].

After the breakdown of the weak spots in the surface layer at a given geometric current density, i_g, an initial active surface area, $S_i = (1 - \theta_p)S_g$, may be directly exposed to the electrolyte, where θ_p represents the passivated fraction of the geometric surface area, S_g, of the lithium electrode. Hence, if the anodic dissolution proceeds unhindered at the bottom of each hole without changing the active surface area, a classical pitting-type anodic dissolution of the electrode can be observed. But for the studied system, Li is well known to react strongly with the $SOCl_2/LiAlCl_4$ electrolyte and to form insoluble decomposition products, such as LiCl microcrystals, the solubility of which are low enough to be neglected (between 1.6×10^{-7} and 2.2×10^{-6} M) [10, 11]. Consequently, the bottoms of the holes, initially put in contact with the electrolyte, can be immediately and partially blocked over a fraction, θ_b, covered by these decomposition products, so that the remaining active surface area, S_r, of the lithium electrode is reduced to $S_r = (1 - \theta_p)(1 - \theta_b)S_g$. Moreover, despite its high solubility, the precipitation of the solute $LiAlCl_4$ can occur rapidly during the anodic dissolution because of the lack of natural convection at the hole bottoms which is not able to homogenize the concentration of cations produced by the high effective current density $i_e = i_g/(1 - \theta_p)(1 - \theta_b)$. By considering that the hole bottoms are partially blocked by the insoluble decomposition and precipitation products, it is conceivable that these products must hamper the lithium discharge in such a way that the blocked fraction, θ_b, increases with the effective current density, i_e. Thereby, the observed diffusion process can be related to an ionic concentration gradient located in the pore holes and closely connected to the formation of insoluble products in the pores.

Due to the permanent renewal of active and passive zones corresponding to the random formation and passivation of holes through the surface layer, the fractions θ_p and θ_b characterize the time-averaged electrode situation during the anodic dissolution.

By considering the initial active surface area, $(1 - \theta_p)$, the geometric current density i_g can be defined by

$$i_g = i_F(1 - \theta_p) \quad (1)$$

where i_F is the Faradaic current density.

By taking into account the remaining non-blocked surface area, $(1 - \theta_b)$, at the pore bottoms, the Faradaic current density, i_F, can be expressed as follows

$$i_F = FK(1 - \theta_b) \quad (2)$$

where F is the Faraday constant, and K is the electrochemical reaction rate as a function of the electrode potential, E.

For simplicity, the ionic concentration, c_0, at the hole bottoms ($z = 0$), for a time-averaged situation, can be assumed to be a linear function of the blocking fraction, θ_b, so that

$$c_0 = c_s\theta_b + c_*(1 - \theta_b) \quad (3)$$

where c_s is the saturation concentration of the solute, and c_* is the bulk concentration of the considered electrolyte solution, such that $c_* < c_0 < c_s$. At the equilibrium potential, c_0 is equal to c_* for open holes ($\theta_b = 0$), while during anodic polarization c_0 tends towards c_s for entirely blocked holes ($\theta_b = 1$). The time-independent Equation 3 implies that the blocked fraction, θ_b, and the ionic concentration, c_0, always vary in phase when a variation of potential E is imposed to the electrode. Such a situation can be valid for the 'complete solution', but not for the 'normal solution' where the diffusion process was observed to be slower than the passivation process.

The concentration c of the Li^+ ions at a distance z from the electrode surface is determined by Fick's second law:

$$D\,\partial^2 c/\partial z^2 = \partial c/\partial t \quad (4)$$

where D is the diffusion coefficient of the lithium ions.

By considering a diffusion length, δ (which can be lower than or equal to the thickness, L, of the surface layer), Equation 4 must satisfy the following boundary conditions:

$$z \geqslant \delta \qquad c = c_* \quad (5)$$

$$z = 0 \qquad c = c_0 \quad (6)$$

According to Fick's first law, the electrochemical rate constant, K, and the Faradic current density, i_F, are given by the following equations:

$$K = -D\{dc/dz\}_{(z=0)} \quad (7)$$

$$i_F = -FD(1 - \theta_b)\{dc/dz\}_{(z=0)} \quad (8)$$

Assuming a linear concentration gradient (Nernst hypothesis), the steady state concentration profile (see Fig. 4b) is given by

$$-dc/dz = (c_0 - c_*)/\delta \quad (9)$$

From Equation 7 the steady state concentration, c_0, at the hole bottoms can be expressed as:

$$c_0 = c_* + K\delta/D \quad (10)$$

With increasing current density, such a concentration can increase from c_* to c_s because of the potential dependence of the rate constant K (variations of the diffusion length δ and the diffusion coefficient D are also possible with the polarization conditions). At the same time, according to Equation 3, the blocked fraction, θ_b, of the pore bottoms will increase.

The dynamic behavior for an angular frequency, ω, can be studied when the system is perturbed by a sine electrode potential

$$\Delta E \exp(j\omega t)$$

of small amplitude, where j is the complex number $\sqrt{-1}$. A corresponding sine Faradaic current density

$$\Delta i_F \exp(j\omega t + \phi)$$

is obtained with a phase difference, ϕ. From Equation 2, the Faradaic impedance, Z_F, of the system implies the relaxation of the blocked fraction, θ_b, of the electrode surface area:

$$1/Z_F = \frac{\Delta i_F}{\Delta E} = \left(\frac{\partial i_F}{\partial E}\right)_{\theta_b} + \left(\frac{\partial i_F}{\partial \theta_b}\right)_E \frac{\Delta \theta_b}{\Delta E} \quad (11)$$

where the first term represents the inverse of the charge transfer resistance, R_t, expressed by:

$$1/R_t = \left(\frac{\partial i_F}{\partial E}\right)_{\theta_b} = \frac{i_F}{K}\left(\frac{\partial K}{\partial E}\right) \quad (12)$$

and the second term, which is related to the diffusion impedance, can be developed by using Equations 1 and 3, as follows:

$$\left(\frac{\partial i_F}{\partial \theta_b}\right)_E \frac{\Delta \theta_b}{\Delta E} = \frac{i_F}{(1 - \theta_b)(c_s - c_*)} \frac{\Delta c_0}{\Delta E} \quad (13)$$

For simplicity, the possible potential dependences of the diffusion length, δ, and the diffusion coefficient, D, will be disregarded. For such a simplified situation [12], integrating Equation 4, according to the boundary conditions given in Equations 4 and 5, yields the following equation:

$$\frac{\Delta c_0}{\left\{\frac{\partial \Delta c}{\partial z}\right\}_{(z=0)}} = -\frac{\delta \tanh \sqrt{j\omega\delta^2/D}}{\sqrt{j\omega\delta^2/D}} \quad (14)$$

Differentiating Equation 7 leads to:

$$\frac{\partial K}{\partial E} \Delta E = -D \left\{\frac{\partial \Delta c}{\partial z}\right\}_{(z=0)} \quad (15)$$

Combining Equations 14 and 15 with Equations 1 and 12 yields:

$$\frac{\Delta c_0}{\Delta E} = \frac{\delta}{R_t F(1 - \theta_b)D} \frac{\tanh \sqrt{j\omega\delta^2/D}}{\sqrt{j\omega\delta^2/D}} \quad (16)$$

From Equations 11, 12, 13 and 16, the Faradaic impedance Z_F can be written as follows:

$$Z_F = R_t \left\{1 - \frac{i_F \delta}{FD(1 - \theta_b)^2(c_s - c_*)} \times \frac{\tanh \sqrt{j\omega\delta^2/D}}{\sqrt{j\omega\delta^2/D}}\right\}^{-1} \quad (17)$$

If the breakdown of the weak spots in the surface layer is considered to be a very fast process, the possible variation of the passivated fraction, θ_p, does not induce any relaxation process. Accordingly, Z_F can be finally expressed as a function of the geometric current density, i_g, by using Equation 1, so that:

$$Z_F = R_t \left\{1 - \frac{i_g \delta}{FD(1 - \theta_p)(1 - \theta_b)^2(c_s - c_*)} \times \frac{\tanh \sqrt{j\omega\delta^2/D}}{\sqrt{j\omega\delta^2/D}}\right\}^{-1} \quad (18)$$

It is noteworthy that this Faradaic impedance, Z_F, does not have the classical form due to a series coupling between a charge transfer process and an ionic diffusion process

$$Z_F = R_t + Z_d$$

where the diffusion impedance, Z_d, is usually defined by the diffusion resistance, R_d, and written as a function of the angular frequency, ω, such as

$$Z_d = R_d \tanh \sqrt{j\omega\delta^2/D} / \sqrt{j\omega\delta^2/D}$$

However, from the analysis of Equation 18, it can be stated that:

– for ω tending to infinity (so that $\tanh \sqrt{j\omega\delta^2/D}$ is equal to unity), the second term of this equation appears as $(1 - \varepsilon)^{-1}$ which is practically equal to $(1 + \varepsilon)$ when ε is an infinitesimal quantity. Accordingly, the Faradaic impedance, Z_F, behaves as a Warburg impedance, Z_w, which is expressed as

$$Z_w = (1 - j)\sigma_\omega^{-1/2}$$

where σ is the Warburg constant given by:

$$\sigma = \frac{R_t i_g}{F\sqrt{2D}(1 - \theta_p)(1 - \theta_b)^2(c_s - c_*)} \quad (19)$$

– for ω tending to zero (so that the ratio $\tanh \sqrt{j\omega\delta^2/D} / \sqrt{j\omega\delta^2/D}$ is equal to unity), Z_F tends to the polarization resistance, R_p, given by:

$$R_p = R_t \left\{1 - \frac{i_g \delta}{FD(1 - \theta_p)(1 - \theta_b)^2(c_s - c_*)}\right\}^{-1} \quad (20)$$

which can be considered as a result of the charge transfer resistance, R_t, placed in series with an equivalent diffusion resistance, R_d, such as:

$$R_d = \frac{R_p i_g \delta}{FD(1 - \theta_p)(1 - \theta_b)^2(c_s - c_*)} \quad (21)$$

Thereby, combining Equations 19 and 21 leads to the determination of the diffusion length, δ, and the diffusion coefficient, D, characteristic of the diffusion process taking place in the pore holes:

$$D(1 - \theta_p)^2(1 - \theta_b)^4 = \frac{1}{2}\left\{\frac{R_t i_g}{F\sigma(c_s - c_*)}\right\}^2 \quad (22)$$

$$\delta(1 - \theta_p)(1 - \theta_b)^2 = \frac{R_d R_t^2 i_g}{2R_p F\sigma^2(c_s - c_*)} \quad (23)$$

Table 1. Variation of the characteristic quantities of the diffusion process as functions of the current density for the case of the 'complete solution' (with SO_2 and $LiAl(SO_3Cl)_4$)

i_g (mA cm^{-2})	$D(1 - \theta_p)^2(1 - \theta_b)^4$ (cm^2 s^{-1})	$\delta(1 - \theta_p)(1 - \theta_b)^2$ (cm)
1	0.4×10^{-13}	1.2×10^{-8}
5	3.8×10^{-13}	2.5×10^{-8}
10	8.6×10^{-13}	2.9×10^{-8}

Table 2. Value ranges of the diffusion coefficient, D, *and the ratio* $(1 - \theta_p)(1 - \theta_b)^2$ *for likely values of the diffusion length,* δ, *at different current densities for the case of the 'complete solution' (with* SO_2 *and* $LiAl(SO_3Cl)_4$*)*

i_g (mA cm^{-2})	$\delta = 1 \times 10^{-3}$ cm		$\delta = 5 \times 10^{-4}$ cm		$\delta = 1 \times 10^{-4}$ cm	
	$(1 - \theta_p)(1 - \theta_b)^2$	D (cm^2 s^{-1})	$(1 - \theta_p)(1 - \theta_b)^2$	D (cm^2 s^{-1})	$(1 - \theta_p)(1 - \theta_b)^2$	D (cm^2 s^{-1})
1	1.2×10^{-5}	2.6×10^{-4}	2.4×10^{-5}	6.4×10^{-5}	1.2×10^{-4}	2.6×10^{-6}
5	2.5×10^{-5}	6×10^{-4}	5×10^{-5}	15×10^{-5}	2.5×10^{-4}	6×10^{-6}
10	2.9×10^{-5}	10×10^{-4}	5.8×10^{-5}	25×10^{-5}	2.9×10^{-4}	10×10^{-6}

5. Discussion

According to the above kinetic model, an evaluation of the parameters related to the diffusion process observed during the anodic polarization in the 'complete solution' can be obtained. To this end, it is necessary to consider a saturation concentration, c_s, of about 5 M for $LiAlCl_4$ in $SOCl_2$, and to suppose that the Warburg constant, σ, remains at a constant value of 250 ohm cm^2 s$^{-1/2}$ for any polarization conditions. As shown in Table 1, the quantities given by Equations 22 and 23 can be calculated from the experimental values of the resistances R_t, R_d and R_p, obtained for different current densities.

In the absence of any experimental data about the ratios $(1 - \theta_p)$ and $(1 - \theta_b)$ which probably depend on each other and vary with the polarization conditions, an estimation of the diffusion coefficient, D, can be obtained only from a presumed value of the diffusion length, δ. Considering that the diffusion process takes place along the pores through the surface layer, it seems reasonable to estimate that the maximum value at δ does not exceed the minimum value of the layer thickness. Such a thickness of the surface layer has been estimated to be about 1×10^{-3} cm after 1 month storage of the lithium electrode in the 'complete solution' (with SO_2 and $LiAl(SO_3Cl)_4$) [5, 6]. As shown in Table 2, the values of D have been calculated for limit values of δ between 1×10^{-4} and 1×10^{-3} cm at different current densities. For example, for δ equal to 5×10^{-4} cm, the value range of D from 6×10^{-5} to 2.5×10^{-4} cm^2 s supports the hypothesis concerning the cation diffusion in the electrolyte. But the relatively high values of D suggest that the ion transport in the pore electrolyte also implies a migration process which has been disregarded in the present model. However, with this simplified model based on a diffusion process hindered by the decomposition and precipitation products in the pores, it is possible to account for the main features observed on the impedance diagrams during the anodic discharge of the lithium electrode in the 'complete solution'. In addition, the low values of the ratio $(1 - \theta_p)(1 - \theta_b)^2$, as shown in Table 2, indicate that only a small percentage of the geometric surface area is active on the lithium electrode.

Such a simplified model does not apply to the case of the 'normal solution' (with only SO_2) essentially for two reasons: (i) a Warburg diffusion process is not in evidence; (ii) the charge transfer resistance, R_t, cannot be determined, a situation which means that the time-independent Equation 3 is not valid because the precipitation does not occur in phase with the variation of the ionic concentration, c_0. A delayed variation in c_0 when the blocked fraction, θ_b, changes with the potential, E, is probably related to the voltage delay effect observed under nonlinear conditions during the discharge of the lithium electrode in this 'normal solution'.

6. Conclusion

The study of the discharge of the Li electrode in the $SOCl_2/LiAlCl_4$-based electrolytes was performed to analyze the elementary processes involved by the inorganic additives SO_2 and $LiAl(SO_3Cl)_4$ used for an effective alleviation of the voltage delay effect.

In the 'complete solution' (with SO_2 and $LiAl(SO_3Cl)_4$), the impedance analysis gives evidence of the rate determining influence of a diffusion process on the kinetic behaviour of the lithium electrode. The results can be explained by a kinetic model based on the assumption that the diffusion of the lithium ions is hindered by the precipitation of the solute $LiAlCl_4$ at the bottom of holes formed inside the LiCl surface layer. The formation of holes through the surface layer is assumed to be due to a dissolution dilation mechanism which allows an ionic diffusion process to occur without any delay from the precipitation of the solute. Then, it has been shown that the impedance data can be explained by a concentration gradient of the lithium ions in the electrolyte present in the pore holes of the surface layer, the remaining active surface area representing only a small percentage of the geometric surface area of the lithium electrode.

In the 'normal solution' (with only SO_2), a more complex coupling between the elementary processes appears to be related to a delay between the ionic diffusion process and the precipitation of the solute in the holes formed through the surface layer. Such a phenomenon is probably at the origin of the voltage delay effect adversely affecting the performances of the Li/$SOCl_2$ primary batteries used without any inorganic additives.

References

[1] V. O. Cantazarite, U.S. Patent 4170693 (Oct. 1979).
[2] N. A. Fleischer and R. J. Ekern, *J. Power Sources* **10** (1983) 179.
[3] W. Bowden, J. S. Miller, D. Cubbison and A. N. Dey, *J. Electrochem. Soc.* **131** (1984) 1768.

[4] D. Vallin and P. Chenebault, in 'Proc. 32th Power Sources Symp.', Cherry Hill (1986).
[5] P. Chenebault, D. Vallin, J. Thevenin and R. Wiart, *J. Appl. Electrochem.* **18** (1988) 625.
[6] P. Chenebault, D. Vallin, J. Thevenin and R. Wiart, Proc. 172nd Electrochem. Soc. Meeting, Honolulu, Hawai (1987).
[7] A. N. Dey, *Electrochim. Acta* **21** (1976) 377.
[8] W. K. Istone and R. J. Brodd, *J. Electrochem. Soc.* **131** (1984) 2467.
[9] B. V. Ratnakumar and S. Sathyanarayana, *J. Power Sources* **10** (1983) 219.
[10] W. P. Hagan and N. A. Hampson, *Electrochim. Acta* **132** (1987) 1787.
[11] M. Salomon, *J. Electrochem. Soc.* **128** (1981) 233.
[12] M. Sluyters-Rehbach and J. H. Sluyters, in 'Electroanalytical Chemistry' (edited by A. J. Bard), Marcel Dekker, New York (1970) Vol. 4, p. 1.